

Experimental and Numerical Free Vibration Analysis of Hybrid Stiffened Fiber Metal Laminated Circular Cylindrical Shell

A. Nazari¹, K. Malekzadeh^{2,*}, A.A. Naderi³

¹Department of Aerospace Engineering, Aerospace Research Institute, Tehran, Iran

²MalekAshtar University, Tehran, Iran

³Faculty of Mechanical Engineering, Emam Ali University, Tehran, Iran

Received 1 November 2018; accepted 2 January 2019

ABSTRACT

The modal testing has proven to be an effective and non-destructive test method for estimation of the dynamic stiffness and damping constant. The aim of the present paper is to investigate the modal response of stiffened Fiber Metal Laminated (FML) circular cylindrical shells using experimental and numerical techniques. For this purpose, three types of FML-stiffened shells are fabricated by a specially-designed method and the burning examination is used to determine the mechanical properties of them. Then, modal tests are conducted to investigate the vibration and damping characteristics of the FML-stiffened shells. A 3D finite element model is built using ABAQUS software to predict the modal characteristics of the FML-stiffened circular cylindrical shells with free-free ends. Finally, the achievements from the numerical and experimental analyses are compared with each other and good agreement has been obtained. Modal analyses of the FML-stiffened circular cylindrical shells are investigated for the first time in this paper. Thus, the results obtained from this study are novel and can be used as a benchmark for further studies.

© 2019 IAU, Arak Branch. All rights reserved.

Keywords: Free vibration; FML-stiffened shell; Modal test; Experimental study.

1 INTRODUCTION

TWO decades ago, Fiber Metal Laminated (FML) shells were created based on the idea of using thin metal layers with fiber reinforced composites. Now, the FML shells have many applications in high-performance engineering due to their high specific strength, high specific stiffness, fatigue resistance, stiffness ductility and impact and damage tolerance. Stiffened composite cylindrical shells are favorable to be used in various branches. They are cylinders reinforced with different types of stiffening structures on the inner, outer or both sides of the shell. These stiffeners significantly increase the load resistance of a cylinder without much increase in weight. The selection of stiffener configuration depends on several factors such as the loading condition, cost, etc. Cylindrical shells composed of FML materials are well known structures in many engineering fields, especially aerospace industry. These shells are often subjected to dynamic loads. Increasing demands of safety of engineering structures,

*Corresponding author. Tel.: +98 21 44659462; Fax: +98 21 44659462.
E-mail address: kmalekzadeh@mut.ac.ir (K. Malekzadeh).

especially where the dynamic load is involved; require better understanding of dynamic properties and response of structures. Finding structural dynamic properties -often including natural frequencies, mode shapes and damping ratios- is highly important in the prediction of structural behavior. Therefore, considering vibration response of the structure is necessary in design process. Modal testing can be performed to determine the dynamic characteristics of existing structures.

A great number of investigations have been emerged rapidly during the past decades concerning the free vibrational analysis of composite cylindrical shells. Many notable numerical and subsequent experimental contributions on the vibration of the laminated structure with and without longitudinal and circumferential stiffeners have been discussed in [1-8]. There are also some good reviews on the vibration of composite shells using experimental and numerical techniques in the following lines. Ganapathiet et al. [9] studied free vibration and transient dynamic response of laminated cross-ply cylindrical shells using FEM method based on higher order theory. Ferreira et al. [10] find the natural frequencies of doubly curved cross ply composite shells using the first order theory of Donnell. Alibeigloo [11] investigated static and free vibration behavior of anisotropic laminated cylindrical shell with various end conditions using differential quadrature method.

An excellent review of researches in this area was collected by Torkamani et al. [12]. They presented a study based on Donnell-type nonlinear strain-displacement relations along with the smearing theory to model the structure. Then the principle of virtual work used to analyze the free vibration of the stiffened shell and different examples solved to validate the scaling numerically and experimentally. Khalili et al. [13-14] investigated free vibration of homogeneous isotropic circular cylindrical shells based on a new three-dimensional refined higher-order theory and studied the Dynamic response of pre-stressed Fiber Metal Laminate circular cylindrical shells subjected to lateral pressure pulse loads. Zhao et al. [15] used a layer-wise theory to analyze the natural frequency and vibration modal of the composite laminated plate. At the same time, experimental method used in this paper to acquire the natural frequencies and vibration modal of a simply supported composite laminated plate. Carrera et al. [16] used Higher-order one dimensional model based on the Carrera Unified Formulation (CUF) to model panels, stringer, and ribs by referring to a unique model.

Recently, Hasan Koruk et al. [17] investigated the natural frequencies and modal loss factors of a cylindrical shell using analytical and computational methods. They identified the sources of damping mechanisms. Shakouri et al. [18] performed experimental and numerical investigation to assess the vibrational behavior of the two joined isotropic conical shells. Governing equations were obtained using thin-walled shallow shell theory of Donnell and Hamilton's principle. The effects of semi-vertex angles and meridional lengths on the natural frequency and circumferential wave number of joined shells were investigated in their study. Attabadi et al. [19] investigated vibration behavior of orthotropic cylindrical shells with variable thickness Based on linear shell theory and applying energy method.

In their study the effects of variable thickness along axial and circumferential directions of the shell on its frequency parameter studied and compared against each other. Hemmatnezhad et al. [20] studied the vibration characteristics of stiffened composite cylindrical shells using experimental, numerical and analytical techniques. They used a specially-designed based on filament winding method to fabricate the specimens from continuous glass fiber and the theoretical formulation established based on Sanders' thin shell theory. In order to validate the analytical achievements, experimental modal analysis conducted on a stiffened cylinder. Results confirm the accuracy of the analytical method. Rahimi et al. [21] applied a unified analytical approach to investigate the vibrational behavior of grid-stiffened cylindrical shells with different boundary conditions. Theoretical formulation established based on Sanders' thin shell theory. The Influences of variations in shell geometrical parameters, boundary condition, and changes in the cross stiffeners angle on the natural frequencies studied. Biswal et al. [22] presented a procedure for investigations numerical and experimental of free vibration behavior of woven fiber Glass/Epoxy laminated composite shells subjected to hydrothermal environments. They considered a composite doubly curved shell model based on first order shear deformation theory. The numerical and experimental results show that there is a reduction in natural frequency of laminated composite shells with the increase in temperature and moisture concentrations. Yang et al. [23] conducted a modal testing to investigate the vibration characteristics of such composite corrugated sandwich cylindrical shells with free-free boundary condition. In order to predict the structural vibration damping, a finite element model combined with modal strain energy approach developed, which is adequately consistent with the experimental results. Torabi et al. [24] studied the effects of delamination size and its thickness-wise and length wise location on the vibration characteristics of cross ply laminated composite beams. Free and constrained mode models introduced and compared in the analytical and finite element methods for the first three modes and a comprehensive discussion among these results is done. To verify the results, modal tests were carried out on the delaminated specimens.

The effect of delamination on the free vibration behavior of the laminated composite curved panels of different geometries (cylindrical, spherical, elliptical, hyperboloid and flat) investigated by Hirwani et al. [25]. The desired governing equation obtained with using classical Hamilton's principle and discretized with the help of finite element steps. El-Helloty [26] investigated the effect of stiffener configuration, number of layers and boundary conditions on the free vibration response of stiffened laminated composite plates with respect to natural frequencies and mode shapes. Comparative study conducted to investigate the effect of stiffener configuration, number of layers and boundary conditions on the free vibration response of stiffened laminated composite plates using the finite element system ANSYS16. Minh Tu et al. [27] investigated free vibration of rotating FGM cylindrical shells with orthogonal stiffeners based on Love's theory. Circumferential wave numbers, the shell length to radius and the shell radius to thickness ratio on the natural frequencies were considered in their study. Garcia et al. [28] considered the vibration behavior of GFRP composites reinforced with nylon nano-fibres experimentally and numerically using a finite element model. Qina et al. [29] extended the IGA approach to solve the free vibration problem of curvilinear stiffened cylindrical and shallow shells. The First-order Shear Deformation Theory (FSDT) and the Reissner-Mindlin shell theory used to model the shells, and the three-dimensional curved beam theory employed to model the stiffener which can be placed anywhere within the shell.

The number of publications performed on the experimental modal analysis of FML shell is scarce, especially with stiffener used in this study. Finding vibrational behavior of this kind of FML shells is a critical task because the dynamic parameters such as the dynamic stiffness and inherent damping value of their components are very important in compliant structures. The modal testing has proven to be an effective and non-destructive test method for estimation of the dynamic stiffness and damping constant of FML shells. Therefore, in this paper, the application of experimental modal testing is demonstrated to assess the natural frequency and damping constant of FML-stiffened shells. A finite element model is built using ABAQUS software, which takes into consideration the numerical results. The specimens under experimental and numerical study in this article are fabricated from glass epoxy and aluminum layers with using a specially designed setup. However, in this study, the vibration behavior of FML-stiffened cylindrical shell is compared with stiffened-composite cylindrical shell. Finally, the effect of using stiffeners and different value of MVF on the free vibration response of stiffened laminated FML circular cylindrical shells is considered.

2 SPECIMENS PREPARATION

Hand lay-up and filament winding are two basic processes for fabricating cylindrical shells. In this study, a specially-designed filament winding and hand lay-up setup are used to fabricate the FML-stiffened cylindrical shell. The specimens are composed of *E*-glass fiber, aluminum layers and room temperature-curing epoxy resin. An available mandrel of 300 mm length and 150 mm outer diameter and taper of 1 mm in the diameter over its length are used to make the cylindrical shell specimens of 300 mm height and 150 mm inner diameter.

In hand lay-up method, liquid resin is placed along with reinforcement against finished surface of a mandrel. The resin serves as the matrix for reinforcing the glass fibers.

In this study, the stiffeners of the specimens are built with filament winding method; then, the metal and composite layers are placed on the stiffeners with using the hand lay-up method. Before wrapping layers around the cylindrical mandrel, the mandrel surface is thoroughly cleaned with acetone to remove any dust, dirt or rust. Then, one layer of Teflon coated release film is placed over the mold surface of the mandrel and the reference line for 0° in the axial direction of the mandrel on the surface.

Untwisted continuous filament of "*E*" – glass and Epon828/HY matrix are used for preparing the composite layers of cylindrical shell specimens. Then, the aluminum individual layers are placed to give the final laminate and this is accomplished by wrapping each layer individually around the mandrel tightly by hand and pressing with special tools, while staggering the joints of the layer evenly around the circumference. The two ends of the shells are cut flat, parallel and normal to the axis of the cylinder using diamond cutting tool, prior to testing, so as to ensure uniform contact on the specimens.

Each specimen in this study contains 5 plies, two aluminum layers and three fabricated glass-epoxy layers with lay-up [GE 0°/90°, AL, GE 0°/90°, AL, GE 0°/90°]. Moreover, cy219 Resin is used as interlayer to bond the sheets to each other.

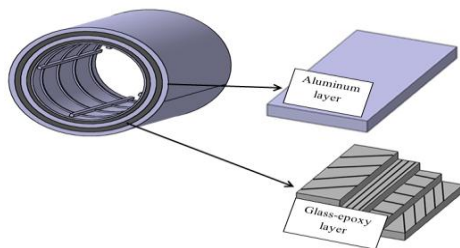
The fibers in the stiffeners are oriented along the length of the stiffeners. The geometry of the under discussion FML-stiffened cylindrical shell is given in Table 1.

Table 1

Geometry properties of the fabricated FML-stiffened shells.

| | Specimen1 | Specimen2 | Specimen3 |
|---|-----------|-----------|-----------|
| Shell height(mm) | 300 | 300 | 300 |
| Shell inner diameter (mm) | 150 | 150 | 150 |
| Shell thickness (mm) | 2 | 2 | 2 |
| Number of aluminum layers | 2 | 2 | 2 |
| Number of glass-epoxy layers | 3 | 3 | 3 |
| Thickness of every aluminum layer(mm) | 0.1 | 0.1 | 0.1 |
| Thickness of every glass-epoxy layer(mm) | 0.6 | 0.6 | 0.6 |
| Number of ring | 4 | 4 | 4 |
| Number of stringer | 4 | 4 | 4 |
| Stiffener cross section(mm ²) | 5×5 | 5×5 | 5×5 |

The schematic view of stacking sequence of the fabricated FML-stiffened circular cylindrical shells is shown in Fig. 1.

**Fig.1**

The schematic view of stacking sequence of the FML-stiffened shells.

As shown in Fig. 2, three numbers of the same specimens are prepared for considering. The end parts are significantly thicker than the middle parts to ensure zero radial displacements along the edges and minimize the risk of local splitting or delamination at the boundaries.

**Fig.2**

Three numbers of the specimens prepared for considering.

In this study, the burning examination and the rule of mixture are used to obtain material properties of the fabricated composite layers of the FML-stiffened shells. The nominal material properties of the FML shell layers are given in Table 2.

Table 2

Mechanical properties of fundamental material.

| material | ρ (kg/m ³) | G_{12} (Gpa) | ν_{12} | E_1 (Gpa) |
|-----------------|-----------------------------|----------------|------------|-------------|
| E-Glass | 2440 | 35.42 | 0.2 | 72 |
| Epon828/HY | 1120 | 1.31 | 0.3 | 3.85 |
| Aluminum layers | 2700 | 27.8 | 0.3 | 72.4 |

The geometric relations of stress-strain for the composite shell can be written as:

$$\begin{bmatrix} \sigma_1 \\ \sigma_2 \\ \sigma_{12} \end{bmatrix} = \begin{bmatrix} Q_{11} & Q_{12} & 0 \\ Q_{21} & Q_{22} & 0 \\ 0 & 0 & Q_{66} \end{bmatrix} \begin{bmatrix} \varepsilon_1 \\ \varepsilon_2 \\ \varepsilon_{12} \end{bmatrix} \quad (1)$$

and the material constants in the reduced stiffness matrix $[Q]$ defined as:

$$\begin{aligned}
 Q_{11} &= \frac{E_1}{1-\nu_{12}\nu_{21}} \\
 Q_{12} &= \frac{\nu_{12}E_2}{1-\nu_{12}\nu_{21}} = Q_{21} \\
 Q_{22} &= \frac{E_2}{1-\nu_{12}\nu_{21}} \\
 Q_{66} &= G_{12}
 \end{aligned}
 \tag{2}$$

where E_1 and E_2 are the elastic modules, G_{12} is the shear modules, ν_{12} and ν_{21} are the poison's ratios. The mechanical properties relations of composite layers for fabricated FML shell can be written as:

$$\begin{aligned}
 E_1 &= E_f V_f + E_m V_m \\
 \nu_{12} &= \nu_{12} V_f + \nu_{21} V_m \\
 E_2 &= \frac{E_f E_m}{V_f E_m + V_m E_f} \\
 G_{12} &= \frac{G_m G_f}{V_f G_m + V_m G_f}
 \end{aligned}
 \tag{3}$$

where E_f is the elastic module of fiber, E_m is elastic module of matrix, G_f is the shear module of fiber, G_m is shear module of matrix, V_f and V_m are volume percentage of fiber and matrix respectively.

Also in Eq.(3) the volume percentage of fiber (V_f) and matrix (V_m) are written as:

$$\begin{aligned}
 V_f &= \frac{w_f \rho_c}{\rho_f} \\
 V_m &= \frac{w_m \rho_c}{\rho_m}
 \end{aligned}
 \tag{4}$$

Mass density of composite material (ρ_c) is obtained from Eq.(5) with respect to mass density of fiber (ρ_f) and mass density of matrix (ρ_m) that finding from burning examination.

$$\rho_c = \frac{\rho_f \rho_m}{\rho_m w_f + \rho_f w_m}
 \tag{5}$$

Burn examination method is used for identification of properties of the composite layers in the fabricated FML shells. For this purpose, one sample of composite layer is cut from each specimen and these samples are placed in furnace under 600 °C temperature. The results of burning examination are shown in Table 3.

Table 3
Results of burning examination.

| | Mass of sample before burning (gr) | Mass of sample after burning (gr) | Weight percentage of fiber(W_f) |
|-----------|---------------------------------------|--------------------------------------|--|
| Specimen1 | 3.04 | 1.3 | %42.76 |
| Specimen2 | 4.55 | 2.64 | %58.02 |
| Specimen3 | 1.94 | 0.98 | %50.52 |
| Average | 3.18 | 1.64 | 51.57% |

The rule of the mixture is used to obtain the material properties of the fabricated composite layer in the FML shell with respect to the volume percentage of fiber and matrix in Eq.(4) and composite density in Eq.(5). The results of burning examination shown in Table 3., are used for these calculations. The mechanical properties of one composite layer of the fabricated FML shell are given in Table 4.

Table 4
Mechanical properties of one composite layer of fabricated the FML shell.

| $G_{12}(Gpa)$ | $E_2(Gpa)$ | $E_1(Gpa)$ | ν_{12} | V_m | V_f | $\rho_c \left(\frac{kg}{m^3} \right)$ | $\rho_f \left(\frac{kg}{m^3} \right)$ | $\rho_m \left(\frac{kg}{m^3} \right)$ | w_m | w_f |
|---------------|------------|------------|------------|-------|-------|--|--|--|--------|--------|
| 1.93 | 5.65 | 26.74 | 0.2664 | %66.4 | %33.6 | 1590 | 2440 | 1160 | 48.43% | 51.57% |

3 FINITE ELEMENT ANALYSES

For the purpose of comparison, 3-D models are built for the FML-stiffened cylindrical shells using ABAQUS CAE 6.12 finite element analysis software. The stiffeners are assembled into the shell and the interfacing areas are tied together. Therefore, the ribs, stringers and shell become a unique structure. Four ribs and four longitudinal stiffeners are used in the FML-stiffener shell. The quadratic planar elements with 8 nodes (S8R) and quadratic cubic elements with 20 nodes (C3D20R) are used to mesh the shell and ribs, respectively. Then, a local cylindrical coordinate system is defined for each element and the corresponding orthotropic properties are aligned accordingly. Geometry and coordinate system for the FML-stiffened cylindrical shell is shown in Fig. 3.

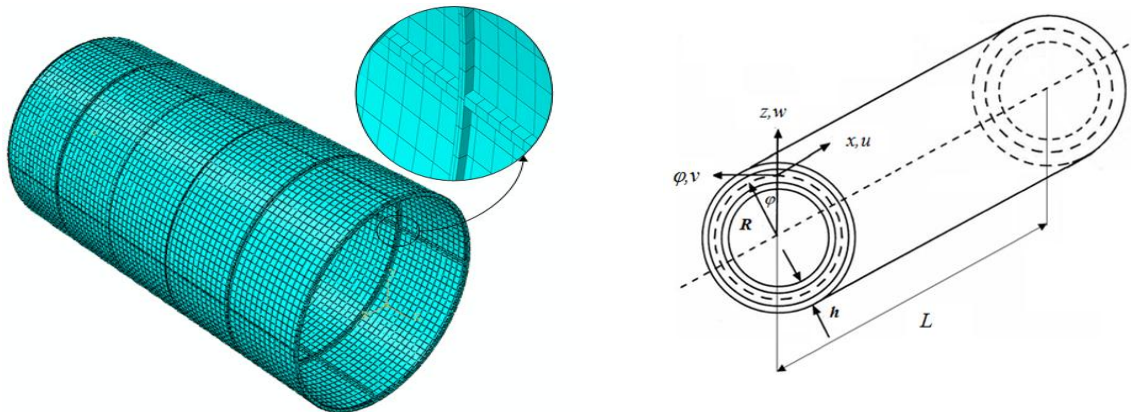


Fig.3
Geometry and coordinate system for the FML-stiffened circular cylindrical shell.

Several different finite-element models with different levels of mesh refinement are developed. Arrangement and type of element scheme change several times to achieve convergent results, and then accurate results are selected. Fig. 4 shows the mesh convergence result obtained from the vibration analysis; the number of element of 10000 is chosen for all the numerical results discussed in this study.

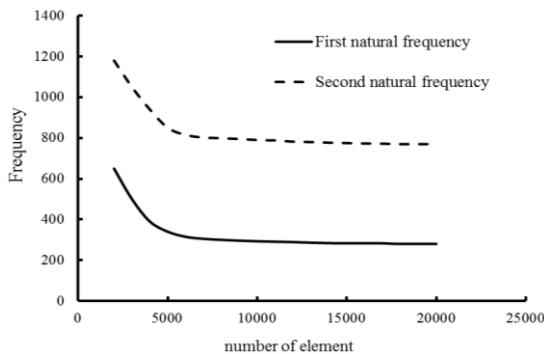


Fig.4
The mesh convergence plot.

4 EXPERIMENTAL MODAL ANALYSES

The modal testing has proven to be an effective and non-destructive test method for estimation of the dynamic stiffness and damping constant. One of the techniques widely used in modal analysis is based on an instrumented hammer impact excitation. By using signal analysis, the vibration response of the structures to the impact excitation is measured and transformed into frequency response function (FRF) using fast Fourier transformation technique.

In this study, a 72 input channel frequency response analyzer, NI PXI-1044, is used for signal acquisition. Since the weights of the test samples are relatively low, the moving mass of the shaker may impose a considerable effect on the natural frequencies of the samples. Therefore, a PCB 086C40 hammer with a force transducer is used for excitation of the samples in 32 points. The sensitivity of the hammer is 2.25 *mv*. However, a PCB 352B10 piezoelectric accelerometer is used for response measurement. The hammer and piezoelectric accelerometer used in this study are shown in Fig. 5.



Fig.5
The PCB 086C40 hammer & the PCB 352B10 piezoelectric accelerometer.

4.1 Extraction of modal properties

Each Frequency Response Function (FRF) is evaluated after averaging over several measurements (3 times) in order to reduce noise. For the experimental modal testing, the structure surface is marked by 32 parallel grid points. Fig. 6 shows the grid points on the outer surface of the FML-stiffened cylindrical shell.

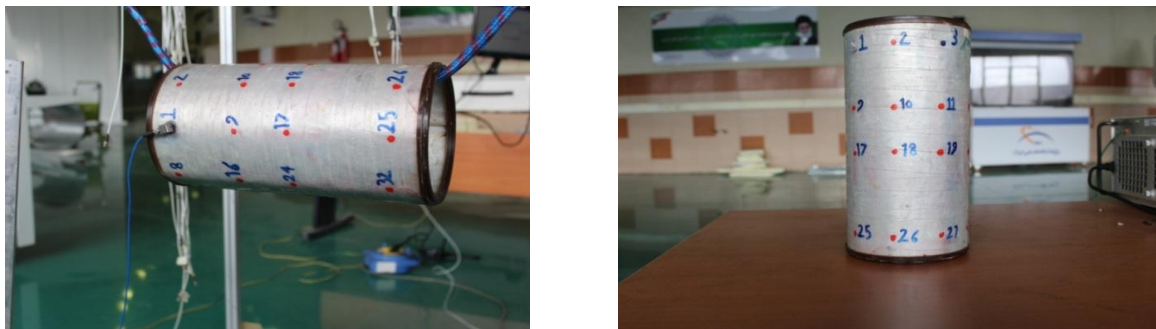


Fig.6
The grid points on the outer surface of the FML-stiffened cylindrical shell.

To simulate the free-free boundary condition, the shell is horizontally hung by flexible strings. Then, modal testing is performed by exciting all the grid points of the structure using a hammer. In fact, modal testing of these shells is much difficult because of its light weight and each additive mass on it can seriously affect the output responses.

Hence, an accelerometer, which is fixed outside the structure at the grid point of number 1, is used to measure the response. The mass of the accelerometer, i.e. 4.5 g, is small in comparison with the mass of test specimens, which is about 460 gr. Finally, MODAL VIEW software is used to process the FRF measurements in order to extract modal parameters and natural frequencies associated to each mode shape by curve fitting FRFs in a specified frequency range.

5 RESULTS AND DISCUSSION

The location of measurement points of the FML shells are shown in Fig.7. Modal parameters of 6 primary modes are extracted through the set of 32 measured FRFs for either of the shell

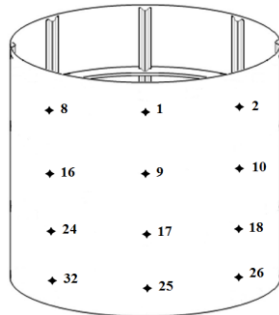


Fig.7
Excitation point.

A number of such plots, the frequency response functions of some distinct points on the FML-stiffened shell, measured during the test are presented in Fig.8. Each peak in this figure indicates at least one natural frequency.

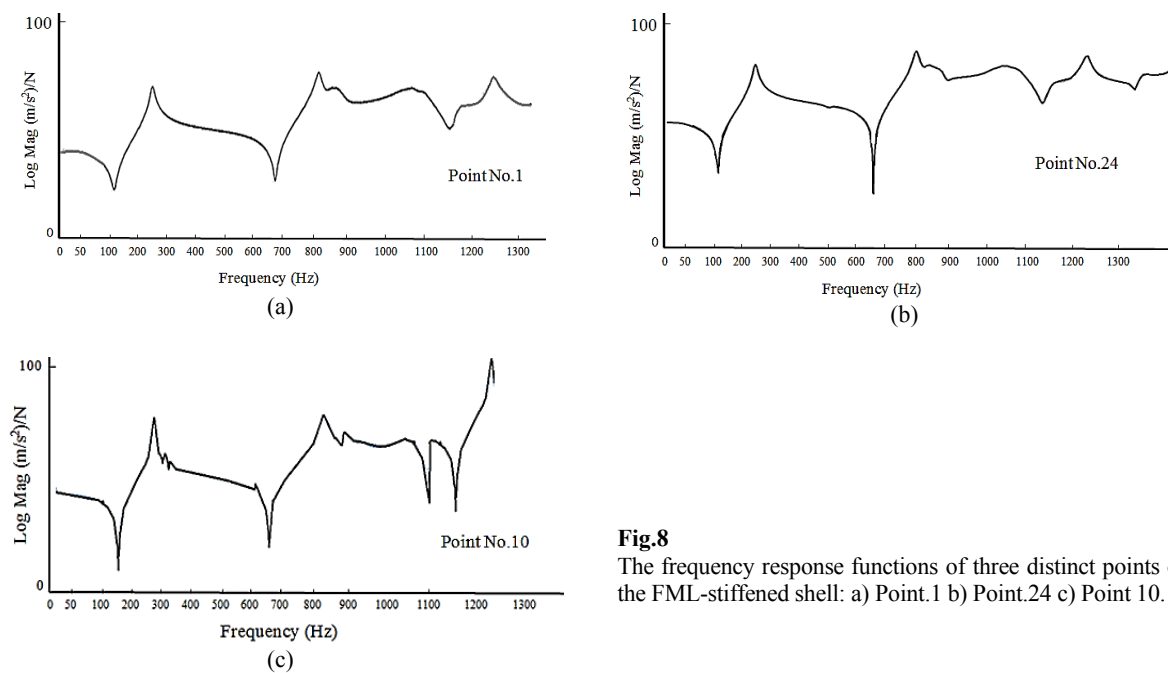


Fig.8
The frequency response functions of three distinct points on the FML-stiffened shell: a) Point.1 b) Point.24 c) Point 10.

The natural frequencies of five distinct points on the FML-stiffened shell for the first three mode numbers, measured during the test modal are presented in Table 5.

Table 5

Experimental natural frequencies measurements at five different grid points of a FML -stiffened cylindrical shell.

| | Point1 | Point9 | Point24 | Point32 | Point10 |
|--------------------------|--------|--------|---------|---------|---------|
| First natural frequency | 295 | 293 | 296 | 295 | 294 |
| second natural frequency | 822 | 823 | 822 | 824 | 820 |
| Third natural frequency | 1220 | 1222 | 1220 | 1226 | 1219 |

The phase and FRF measurements for one grid point of a FML-stiffened shell are plotted in Fig.9.

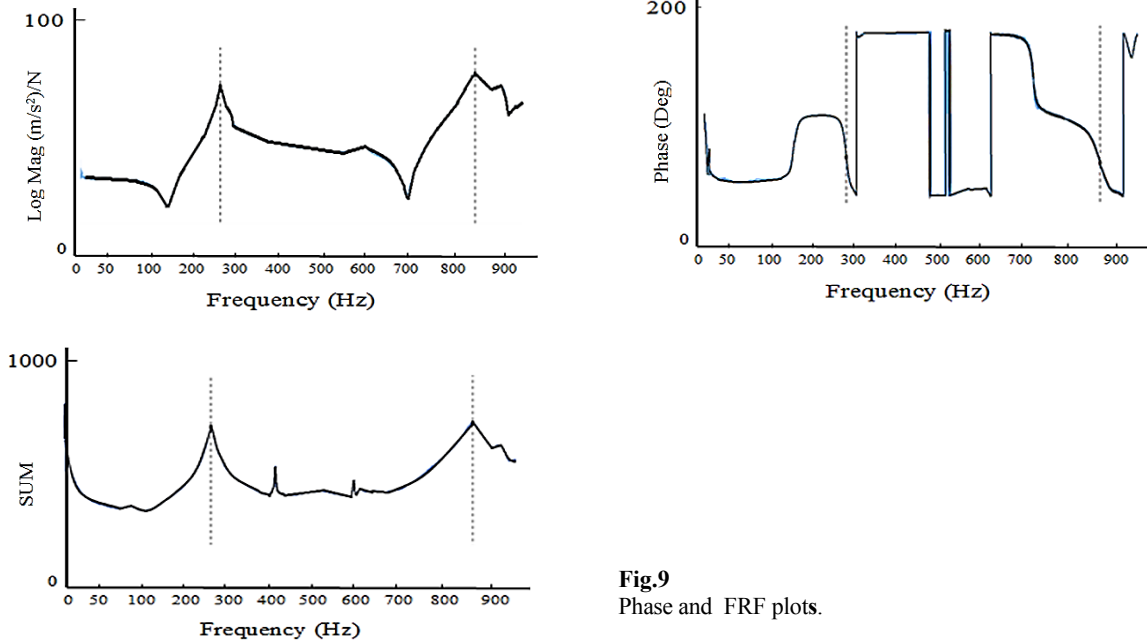


Fig.9
Phase and FRF plots.

The peaks are not clear enough for frequency values greater than 1000 Hz. Moreover, all the peaks in this region do not really indicate the vibration modes but can be of noise signals. This fact is due to the light weight of the fabricated specimens and any possible influence of additive mass caused by the accelerometer. For the aforementioned reasons, the exerted impact cannot excite the vibration modes with higher frequencies. For evaluating the greater natural frequencies, the band cursor width for the mode estimation should be more decreased around any possible peak and the advanced curve fitting methods should be employed.

The mode shapes obtained from modal tests for the first three mode numbers of a FML-stiffened cylinder are presented in Fig.10.

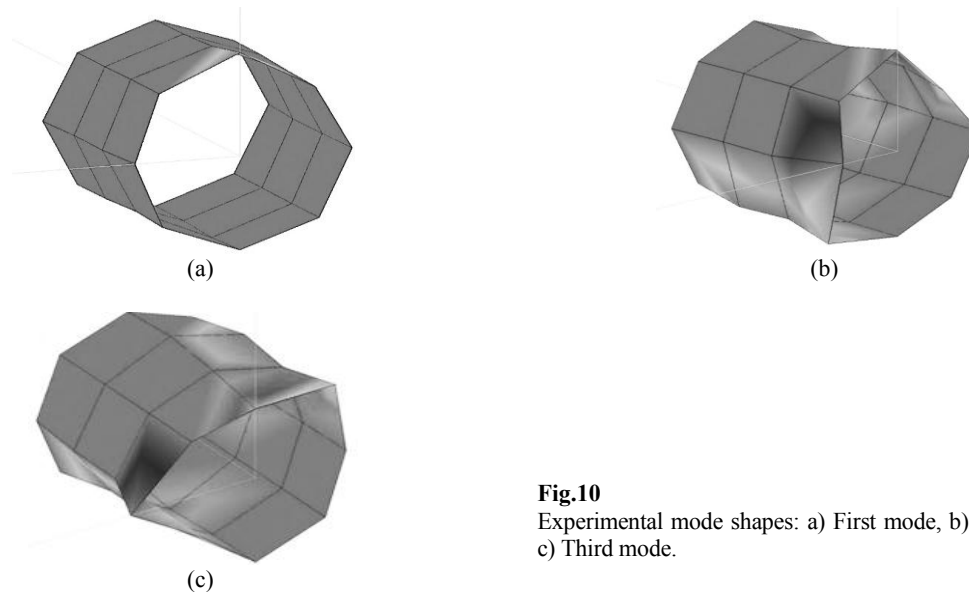


Fig.10
Experimental mode shapes: a) First mode, b) Second mode, c) Third mode.

Mode validation analysis is also performed in order to evaluate the validity of estimated modes from measured FRFs. Here, the most common assurance indicator i.e. modal assurance criterion (MAC) is chosen for the validation. MAC is described as a scalar constant indicating the degree of linearity between one modal and another reference

modal vector. The value range of MAC is from 0, representing linear independent, to 1. The numerical presentation of MAC values for the first six mode numbers of a FML-stiffened cylinder is given in Table 6.

Table6

Numerical presentation of MAC values.

| Mode | 1 | 2 | 3 | 4 | 5 | 6 |
|------|--------|-------|--------|--------|--------|--------|
| 1 | 1 | 0.011 | 0.0071 | 0.0041 | 0.0034 | 0.001 |
| 2 | 0.0025 | 1 | 0.0023 | 0.0015 | 0.0012 | 0.002 |
| 3 | 0.008 | 0.07 | 1 | 0.15 | 0.014 | 0.012 |
| 4 | 0.017 | 0.005 | 0.012 | 1 | 0.019 | 0.009 |
| 5 | 0.142 | 0.016 | 0.014 | 0.003 | 1 | 0.0019 |
| 6 | 0.003 | 0.010 | 0.023 | 0.0121 | 0.002 | 1 |

The 3-D graphical representation of the aforementioned MAC plot is also illustrated by Fig.11.

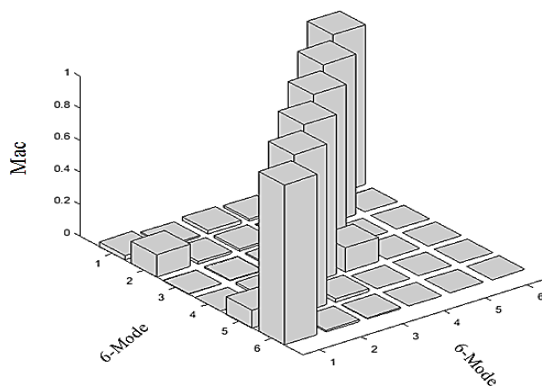


Fig.11
Presentation of MAC values.

Table7., lists the first five natural frequencies of the FML-stiffened circular cylindrical shells achieved via experimental modal analysis (EMA) and finite element analysis (FEA).

Table 7

The first five numerical and experimental natural frequencies of the FML-stiffened cylindrical shells.

| | Mode number (<i>n,m</i>) | Experimental natural frequency (Hz) | Numerical natural frequency (Hz) | Deviation | Experimental damping ratio |
|-----------|-------------------------------|--|-------------------------------------|-----------|-------------------------------|
| Specimen1 | (0,2) | 295 | 284 | 3% | 0.7 |
| | (1,2) | 822 | 770 | 6% | 0.64 |
| | (0,3) | 1220 | 1171 | 4% | 0.64 |
| | (1,3) | 1515 | 1473 | 2% | 0.5 |
| | (2,3) | 1630 | 1545 | 5% | 0.55 |
| Specimen2 | (0,2) | 303 | 284 | 6% | 0.8 |
| | (1,2) | 830 | 770 | 7% | 0.6 |
| | (0,3) | 1250 | 1171 | 6% | 0.7 |
| | (1,3) | 1545 | 1473 | 4% | 0.58 |
| | (2,3) | 1660 | 1545 | 7% | 0.5 |
| Specimen3 | (0,2) | 310 | 284 | 9% | 0.6 |
| | (1,2) | 840 | 770 | 9% | 0.55 |
| | (0,3) | 1190 | 1171 | 1% | 0.43 |
| | (1,3) | 1560 | 1473 | 5% | 0.45 |
| | (2,3) | 1615 | 1545 | 4% | 0.4 |

As can be seen, the natural frequencies obtained from the two types of experimental and numerical analyses meet a good agreement. For some vibration modes, difference between the two types of analyses is more significant. These differences are mainly due to the complexity of the structure, inaccuracies may occur while fabricating the

specimens. This comparison illustrates that the FE model is qualified enough for predicting the vibrational behavior of FML-stiffened composite cylindrical shells.

The first nine corresponding mode shapes of the FML-stiffened cylindrical shell are shown in Fig. 12.

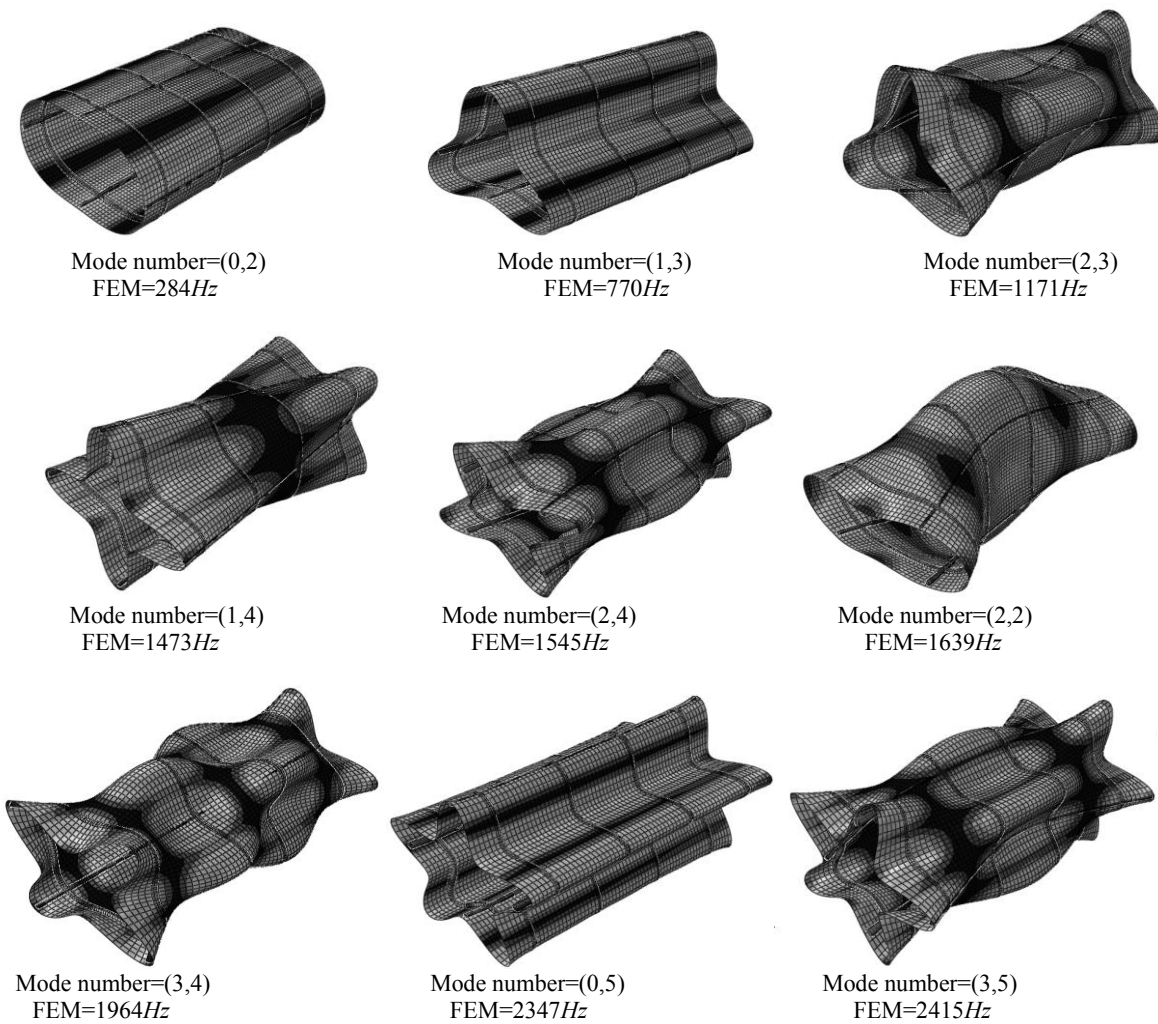


Fig.12

The first nine mode shapes of the FML-stiffened cylindrical shell with free-free boundary condition.

Variation of the lowest natural frequencies against Metal Volume Fraction (MVF) for the FML-stiffened cylindrical shell is shown in Fig.13.

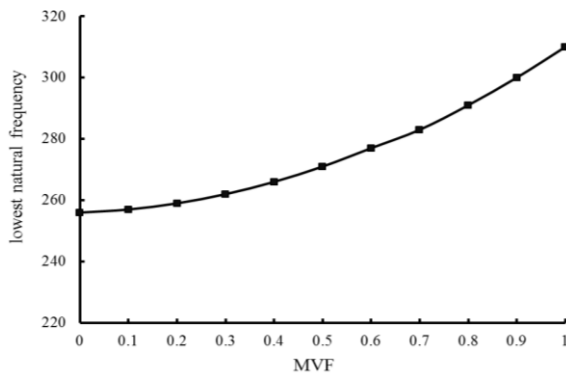


Fig.13

Variation of the lowest natural frequencies against MVF.

As it is clear in this figure, increasing the value of MVF from 0 to 1, causes to increase the lowest natural frequencies of the FML-stiffened shell about 21%. Fig. 14 illustrates the effect of MVF on the variation of the lowest natural frequencies against thickness to radius.

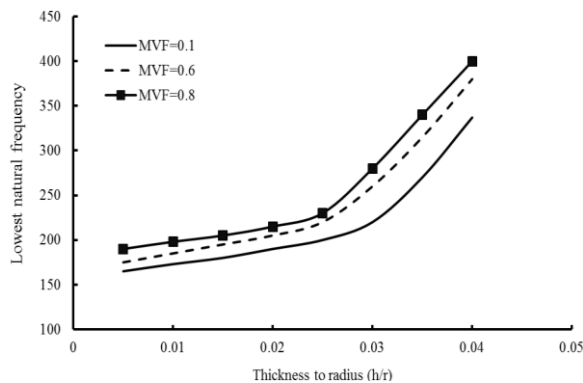


Fig.14
Variation of the lowest natural frequencies against thickness to radius.

As can be seen in Fig. 14, by increasing the thickness to the radius ratio, the relative frequency increases. However, the trends in natural frequencies against h/r graphs are similar for different value of MVF.

In Fig. 15 the natural frequencies of the FML-stiffened cylindrical shell are compared with natural frequencies of the GE-stiffened composite cylindrical shell for different values of the mode numbers. The FML-stiffened shell is considered to be made of three Glass/Epoxy layers and two aluminum layers. The GE-stiffened composite shell consists of five Glass/Epoxy layers. The other geometric parameters of these shells are the same.

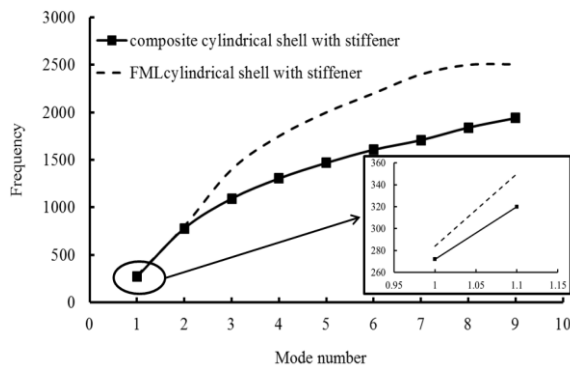


Fig.15
Comparison of the natural frequencies of the FML-stiffened cylindrical shell with the GE-stiffened composite cylindrical shell for different values of the mode numbers.

As can be seen from Fig. 15 in all the mode numbers, the natural frequencies of the FML-stiffened cylindrical shell are more than the natural frequencies of the GE-stiffened composite cylindrical shell. This fact is due to the more stiffness of the FML-stiffened shell in compared to the GE-stiffened composite cylindrical shell. However, the difference in natural frequency between the FML shell and the GE composite shell is not the same in all the mode numbers; this difference is neglected in lower mode numbers while regarded significant in higher mode numbers. The weight of the FML-stiffened and GE-stiffened cylindrical shells is fixed in all the mode numbers while the difference between the two curves becomes greater as the mode number increases. The only reason of this matter is the presence of the aluminum layers in the FML construction, which causes to maintain the stiffness of the FML shells in higher mode numbers. It should be mentioned that the aluminum layers have significant effect on the stiffness of the FML-stiffened cylindrical shells for greater mode numbers.

Table 8., illustrates the mass and first natural frequency of the FML-stiffened and GE-stiffened cylindrical shells.

Table 8

The mass and first natural frequency of the FML-stiffened and GE-stiffened cylindrical shells.

| | First frequency(Hz) | Weight(kg) | Stiffness(N/m) |
|---------------------------------|---------------------|------------|----------------|
| FML-stiffened cylindrical shell | 284 | 0.543 | 43796 |
| GE-stiffened cylindrical shell | 236 | 0.518 | 28850 |

From Table 8., it is observed that the stiffness of the FML-stiffened shell is about 33% more than that of the GE-stiffened cylindrical shell. This is while the mass of the FML shell is only 4% more than that of the GE-stiffened shell. The reason for this is the use of aluminum layers in the FML shells, which causes to increase the stiffness of the shell with faster rate than the shell weight.

The effect of stiffeners on the fundamental natural frequencies of the FML-stiffened cylindrical shells is exhibited in Fig 16. For this purpose, the relationship between frequencies and mode numbers of the stiffened and unstiffened FML shells is investigated.

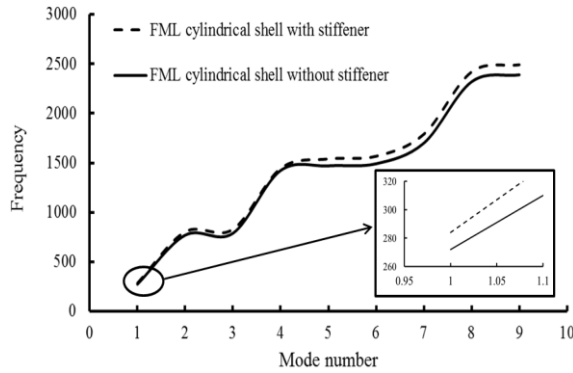


Fig.16 Comparison of the variation of natural frequencies against mode number for the stiffened and unstiffened FML cylindrical shells.

As can be seen in Fig. 16, for both the stiffened and unstiffened FML cylindrical shells, the natural frequencies increase with increasing the mode number. The natural frequencies of the FML-stiffened shells are more than those of the FML-unstiffened cylindrical shells for all the mode numbers. As is observed from Fig. 16, the difference between the natural frequencies of stiffened and unstiffened FML shells becomes greater as the mode numbers increase. This means that, for greater mode numbers, the presence of the grid structure has more significant effect on the vibrational behavior of the FML shells.

Variation of the lowest natural frequency against MVF for the stiffened and unstiffened FML circular cylindrical shells is depicted in Fig. 17.

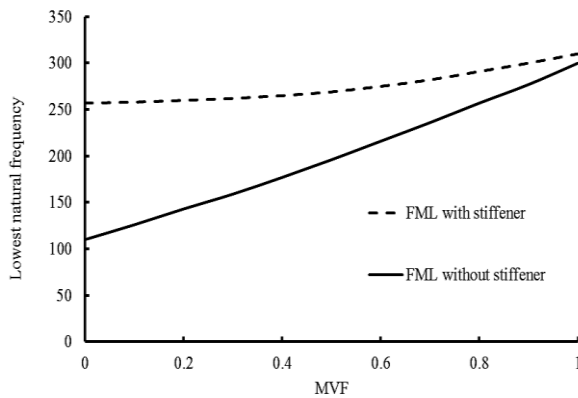


Fig.17 Variation of the lowest natural frequency against MVF for the stiffened and unstiffened FML circular cylindrical shells.

As it is clear in Fig. 17, the difference between the value of the lowest natural frequency of the stiffened and unstiffened FML shells is highest in MVF=0 and lowest in MVF=1.

In MVF=0, the construction of the FML shells consists of only composite layers; therefore, the effect of composite stiffeners on the FML shells stiffness is highest in MVF=0. As a result, the difference between natural frequency of the stiffened and unstiffened FML shells is highest in MVF=0. With increasing the MVF value, the difference between natural frequency of the stiffened and unstiffened FML shells decreases. Because in higher MVF value, the metal layers have more quota in FML construction which cause to decrease the effect of composite stiffener on the stiffness of the FML-stiffened shells. Therefore, the difference between the natural frequency of the stiffened and unstiffened FML shells decreases with increasing the MVF value.

6 CONCLUSIONS

In this article, free vibration characteristics of the FML-stiffened composite cylindrical shells are investigated numerically and experimentally, probably for the first time. The specimens are composed of *E*-glass fibers, aluminum layers and room temperature-curing epoxy resin using a specially designed setup. A series of benchmark tests are carried-out with three similar FML cylindrical shells in order to verify the experimental and numerical results of vibrational analyses. These samples are tested under free-free boundary condition. The experimental results are compared with general finite element program (ABAQUS) results. Some results are achieved which are listed as follows:

- The experimental results are the most important achievement of this study that can be used as a benchmark for further study on this subject.
- Results obtained from the two types of analyses meet a good agreement. The discrepancy between numerical and experimental results is about 5%.
- By using the results of the experimental study, a more accurate numerical model is attempted to be achieved. The differences in some cases are mainly due to the complexity of the structure and errors may occur while fabricating the specimens.
- The average of the first experimental natural frequency of the three fabricated FML shells is equal to 300Hz.
- The natural frequencies of the FML shells increase with increasing the MVF.
- The stiffness of the FML-stiffened shell considered in this study is about 33% more than the stiffness of the GE-stiffened cylindrical shell; while mass of the FML shell is only 4% more than that of the GE-stiffened shell. This point out the fact that the aluminum layers of the FML shells further affect the stiffness of the shell rather than the mass.
- The fundamental natural frequency of the FML shells increases with increasing the thickness to radius ratio for the FML shells with various MVF.
- The natural frequencies of the FML-stiffened cylindrical shell are more than the natural frequencies of the GE-stiffened composite cylindrical shells in all the mode numbers.
- The difference between the natural frequencies of the FML-stiffened cylindrical shell and GE-stiffened composite shell is neglected in lower mode numbers and regarded significant in higher mode numbers. This is because the aluminum layers of the FML shells have more significant effect on the stiffness of the FML cylindrical shell for greater mode number.
- The natural frequencies of the FML-stiffened cylindrical shells are more than the natural frequencies of the FML-unstiffened cylindrical shells in all the mode numbers.
- The difference between natural frequencies of the stiffened and unstiffened FML shells increases with increasing the mode numbers because for greater mode numbers, the presence of the grid structure has more significant effect on the vibrational behavior of the FML shells.
- The difference between the natural frequencies of the stiffened and unstiffened FML shells decreases with increasing the MVF value.
- The metal layers have more quotas in the FML construction in higher MVF, which cause to decrease the effect of composite stiffener on the stiffness of the FML-stiffened shells in high MVFs.

REFERENCES

- [1] Sharma C.B., 1974, Calculation of frequencies of fixed-free circular cylindrical shells, *Journal of Sound & Vibration* **35**: 55-76.
- [2] Mead D.J., Bardell N.S., 1986, Free vibration of a thin cylindrical shell with discrete axial stiffeners, *Sound and Vibration* **111**: 229-250.
- [3] Sharma C.B., Darvizeh M., Darvizeh A., 1996, Free vibration response of multilayered orthotropic fluid-filled circular cylindrical shells, *Composite Structures* **34**: 349-355.
- [4] Wang C.M., Swaddiwudhipong S., Tian J., 1997, Ritz method for vibration analysis of cylindrical shells with ring stiffeners, *Sound and Vibration* **123**: 123-134.
- [5] Gong S.W., Lam K.Y., 2000, Effects of structural damping and stiffness on impact response of layered structures, *AIAA Journal* **38**: 1730-1735.
- [6] Hosokawa K., Murayama M., Sakata T., 2000, Free vibration analysis of angle-ply laminated circular cylindrical shells with clamped edges, *Science and Engineering of Composite Materials* **9**: 75-82.

- [7] Vogelesang L.B., Volt A., 2000, Development of fiber metal laminates for advanced aerospace structure, *Journal of Material Processing Technology* **103**: 1-5.
- [8] Ruotolo R., 2001, A comparison of some thin shell theories used for the dynamic analysis of stiffened cylinders, *Journal of Sound and Vibration* **243**: 847-860.
- [9] Ganapathi M., Patel B.P., Patel H.G., Pawargi D.S., 2003, Vibration analysis of laminated cross-ply cylindrical shells, *Journal of Sound and Vibration* **262**(1): 65-86.
- [10] Ferreira A.J.M., Roque C.M.C., Jorge R.M.N., 2007, Natural frequencies of FSDT cross-ply composite shells by multiquadrics, *Journal of Composite Structure* **77**(3): 296-305.
- [11] Alibeigloo A., 2009, Static and vibration analysis of axi-symmetric angle ply laminated cylindrical shell using state space differential quadrature method, *International Journal of Pressure Vessels and Piping* **86**: 738-747.
- [12] Torkamani S.h., Navazi H.M., Jafari A.A., Bagheri M., 2009, Structural similitude in free vibration of orthogonally stiffened cylindrical shells, *Journal of Thin-Walled Structures* **47**: 1316-1330.
- [13] Khalili S.M.R., Malekzadeh K., Davar A., Mahajan P., 2010, Dynamic response of pre-stressed Fiber Metal Laminate (FML) circular cylindrical shells subjected to lateral pressure pulse loads, *Journal of Composite Structures* **92**: 1308-1317.
- [14] Khalili S.M.R., Davar A., Malekzadeh K., 2012, Free vibration analysis of homogeneous isotropic circular cylindrical shells based on a new three-dimensional refined higher-order theory, *International Journal of Mechanical Sciences* **56**: 1-25.
- [15] Zhao L., Wu J., 2013, Natural frequency and vibration modal analysis of composite laminated plate, *Journal of Advanced Materials Research* **711**: 396-400.
- [16] Carrera E., Zappino E., Filippi M., 2013, Free vibration analysis of thin-walled cylinders reinforced with longitudinal and transversal stiffeners, *Journal of Vibration and Acoustics* **135**: 011019.
- [17] Koruk H., Jason T., Dreyer J.T., Singh R., 2014, Modal analysis of thin cylindrical shells with cardboard liners and estimation of loss factors, *Journal of Mechanical Systems and Signal Processing* **45**: 346-359.
- [18] Shakouri M., Kouchakzadeh M.A., 2014, Free vibration analysis of joined conical shells: Analytical and experimental study, *Thin-Walled Structures* **85**: 350-358.
- [19] Attabadi P.B., Khedmati M.R., Attabadi M.B., 2014, Free vibration analysis orthotropic thin cylindrical shells with variable thickness by using spline functions, *Latin American Journal of Solids and Structures* **11**: 2099-2121.
- [20] Hemmatnezhad M., Rahimi G.H., Tajik M., Pellicano F., 2015, Experimental, numerical and analytical investigation of free vibrational behavior of GFRP-stiffened composite cylindrical shells, *Journal of Composite Structures* **120**: 509-518.
- [21] Rahimi G.H., Hemmatnezhad M., Ansari R., 2015, Prediction of vibrational behavior of grid-stiffened cylindrical shells, *Journal of Advance in Acoustic and Vibration* **73**: 10-20.
- [22] Biswal M., Sahu S.K., Asha A.V., 2015, Experimental and numerical studies on free vibration of laminated composite shallow shells in hygrothermal environment, *Journal of Composite Structures* **127**: 165-174.
- [23] Yang J.S., Xiong J., Ma L., NaFeng L., Yang Wang S., Zhi Wu L., 2016, Modal response of all-composite corrugated sandwich cylindrical shells, *Journal of Composites Science and Technology* **115**: 9-20.
- [24] Torabi K., Shariati-Nia M., Heidari-Rarani M., 2016, Experimental and theoretical investigation on transverse vibration of delaminated cross-ply composite beams, *International Journal of Mechanical Sciences* **115**: 1-11.
- [25] Hirwania C.K., Patila R.K., Panda S.K., Mahapatra S.S., Srivastava L., Buragohain M.K., 2016, Experimental and numerical analysis of free vibration of delaminated curved panel, *Aerospace Science and Technology* **54**: 353-370.
- [26] El-Helloty A., 2016, Free vibration analysis of stiffened laminated composite plates, *International Journal of Computer Applications* **156**: 12-23.
- [27] Minhtu T., Van Loi N., 2016, Vibration analysis of rotating functionally graded cylindrical shells with orthogonal stiffeners, *Latin American Journal of Solids and Structures* **13**: 2952-2962.
- [28] Garcia C., Wilson J., Trendafilova I., Yang L., 2017, Vibratory behavior of glass fibre reinforced polymer (GFRP) interleaved with Nylon Nanofibers, *Journal of Composite Structures* **132**: 6-18.
- [29] Qina X.C., Donga C.Y., Wang F., Gong Y.P., 2017, Free vibration analysis of isogeometric curved linearly stiffened shells, *Journal of Thin-Walled Structures* **116**: 124-135.